Semigeostrophic Flow over Orography in a Stratified Rotating Atmosphere. Part III: Evaluation of a Lee Cyclogenesis Mechanism

BRIAN D. GROSS*

Department of Astrophysical, Planetary, and Atmospheric Sciences, University of Colorado, Boulder, Colorado

(Manuscript received 11 April 1989, in final form 22 August 1989)

ABSTRACT

Three-dimensional, adiabatic, inviscid flow over orography is examined by means of a semigeostrophic model expressed in isentropic coordinates. A nondimensional mountain height $\epsilon/D \leqslant 0.5$, based on the deformation depth $D \sim 3 \times 10^3$ m, and a Rossby number Ro $\leqslant 0.3$, based on the mountain breadth $L \geqslant 3.5 \times 10^5$ m and a constant Coriolis parameter f, provide constraints on the flow field.

Vortex tube stretching is evaluated as a mechanism for lee cyclogenesis. It is shown that the convergence of both planetary and geostrophic relative vorticity filaments enhances geostrophic cyclonic vorticity in a semigeostrophic model. In contrast, ageostrophic cyclonic vorticity is weakened by convergence. These features are illustrated in a numerical simulation of flow over an isentropic isolated mountain. The initial state is characterized by an isolated region of ageostrophic cyclonic vorticity in the lee of the obstacle, accompanied by convergence. A potential vorticity disturbance, associated with an internal cold front and a two-dimensional upper-level jet, is advected over the isolated obstacle. In principle, the coupling of ascending motion ahead of the disturbance with descending motion in the lee provides vortex tube stretching. It is shown that this mechanism *does not* initiate lee cyclogenesis in either a quasi-geostrophic or semigeostrophic model with isentropic boundaries. In particular, horizontal convergence and vertical stretching are significantly diminished by the intrusion of weakly stratified air into the lee. Additionally, the ageostrophic cyclonic vorticity present in the initial state is not effectively enhanced by vortex tube stretching, according to the ageostrophic vorticity theorem for semigeostrophic flow. The absence of both blocking by the obstacle and potential temperature gradients along the lower boundary is suggested as a possible reason for the failure of vortex tube stretching to initiate lee cyclogenesis in the model presented here.

1. Introduction

Cyclogenesis preferentially occurs in the lee of major mountain ranges (Petterssen 1956, p. 267). Lee cyclogenesis has been well documented, observed in the Earth's atmosphere [e.g., Buzzi and Tibaldi 1978; McGinley 1982; and numerous contributors to the Alpine Experiment (ALPEX)], and delineated by means of laboratory experiments (Boyer et al. 1987). However, an accepted theory for this phenomenon has yet to emerge, in part because the historic absence of detailed observations has only recently been remedied by ALPEX.

Smith (1979) has discussed no less than seven theories that may account for the intensification of cyclonic vorticity in the lee of mountains. These include arguments based on transient phenomena (Huppert and Bryan 1976), and the presence of an Ekman layer in the flow (Buzzi and Tibaldi 1977). More recently, Smith (1984) has proposed that lee cyclogenesis may be associated with the first trough of a standing baroclinic lee wave, while Pierrehumbert (1985) and Speranza et al. (1985) have proposed orographic modification of an Eady wave as the principal mechanism of lee cyclogenesis. Numerical models, such as those of Dell'Osso and Radinović (1984), Mattocks and Bleck (1986), and Malguzzi et al. (1987) have successfully developed cyclones in the lee of the Alps, however the physical mechanisms responsible for lee cyclogenesis remain unclear. Indeed, Egger (1988) has shown that the physical mechanisms underlying the so-called "mature" theories of lee cyclogenesis (specifically those of Smith 1984; Pierrehumbert 1985, Speranza et al. 1985) cannot adequately produce a lee cyclone in a primitive equation model. This result certainly calls into question the general applicability of these theories.

One simple mechanism that may promote the rapid intensification of cyclonic vorticity is vortex-tube stretching in the lee of the mountain. An early discussion of this concept is provided by Hess and Wagner (1948). More recently, Chung et al. (1976) and McGinley (1982), among others, have also proposed

* Center for Atmospheric Theory and Analysis, University of Colorado. Current Affiliation: NRC Research Associate, NASA Goddard Space Flight Center.

Corresponding author address: Dr. Brian Gross, Code 611, NASA/GSFC, Greenbelt, MD 20771.

that the leeside stretching of low-level cyclonic vorticity is an important characteristic of lee cyclogenesis. Radinović (1986) and Hu and Reiter (1987) have suggested that the deformation of the thermal structure of the atmosphere by a mountain barrier produces surface cyclonic vorticity according to the thermal wind term in Sutcliffe's (1947) development theory, which is based on the stretching mechanism.

Vortex tube stretching is associated with the divergence term in the vorticity equation (e.g., Dutton 1986, pp. 339–348). Divergence may be associated with atmospheric circulations such as a jet streak (Reiter 1963). In fact, many authors (e.g., Radinović 1965; Smith 1984) have noted that lee cyclogenesis commences with the approach of an upper level trough and jet, and a surface cold front, toward a mountain barrier. This trough may be associated with an upper-level potential vorticity disturbance (Bleck and Mattocks 1984), and Mattocks and Bleck (1986) have numerically simulated lee cyclogenesis when a region of high potential vorticity air approaches an orographic barrier. They conclude that vertical stretching initiates lee cyclogenesis, although a detailed analysis of the stretching mechanism is absent in their discussion.

Unresolved aspects of the vortex stretching theory are the origin of the low-level cyclonic vorticity that is intensified by this mechanism, and the details of the interaction of the trough and cold front with the orography. This latter aspect has been addressed in part by Blumen and Gross (1987a), and by Zehnder and Bannon (1988). One particular mechanism for maintaining cyclonic vorticity in the lee of a mountain has been discussed by Gross and Blumen (1988, hereafter referred to as I). In I, it was shown that the semigeostrophic interaction of a diffluent flow with a mountain anticyclone produces a region of relatively strong leeside *ageostrophic* cyclonic vorticity, accompanied by convergence (see Fig. 9 in I). Further, Chung et al. (1976) have concluded that the majority of lee cyclones form in the presence of cross-barrier diffluent flow, while Radinović (1986) has observed that upper-level diffluent flow is present to some degree in all eight cases of lee cyclogenesis that occurred during the ALPEX Special Observing Period (March–April 1982).

In this presentation, the interaction of an approaching upper-level potential vorticity disturbance with the mountain circulations discussed in I is examined by means of a semigeostrophic model expressed in isentropic coordinates. A nondimensional mountain height $\epsilon/D \leqslant 0.5$, based on the deformation depth $D \sim 3 \times 10^3$ m, and a Rossby number $\mathrm{Ro} \leqslant 0.3$, based on the mountain breadth $L \geqslant 3.5 \times 10^5$ m and a constant Coriolis parameter f, provide constraints on the flow field. The upper-level disturbance consists of a region of high potential vorticity air associated with an internal baroclinic zone. This disturbance is advected in a deformation flow toward an isolated mountain. The present analysis focuses on vortex tube stretching as the *only* mechanism for cyclogenesis.

The stretching mechanism considered here has been described in qualitative terms by McGinley (1982), in a comprehensive diagnosis of Alpine lee cyclogenesis. In the present model, a thermally direct ageostrophic circulation, associated with a potential vorticity disturbance approaching a mountain barrier, is characterized by midlevel rising motion ahead of the disturbance. This is the so-called Sawyer–Elliasen circulation that has been successfully modeled by many authors (e.g., Buzzi et al. 1981). In principle, as the disturbance passes into the lee, this rising motion couples with the descent of air on the lee side of the barrier to produce relatively strong vertical stretching of vortex tubes in the lower half of the flow.

Vortex tube stretching provides the principal mechanism of vorticity enhancement in the present analysis, and is discussed in section 2. A semigeostrophic vorticity theorem is derived in isentropic coordinates. Further, it is shown that vortex tube stretching *does not* enhance the lee-side ageostrophic cyclonic vorticity that is prescribed in the initial state, thereby limiting this mechanism's ability to provide significant vortex spinup. The semigeostrophic model used to evaluate the stretching mechanism is an extension of the isentropic coordinate model of Buzzi et al. (1981), and is presented in section 3. Model results are presented in section 4. In particular, it is verified that significant vortex spin-up is absent in this semigeostrophic model with isentropic boundaries, and a lee cyclone does not form. Differences between the semigeostrophic and quasigeostrophic solutions are analyzed in section 5. Concluding remarks are presented in section 6.

2. Spinup mechanisms

In an adiabatic, isentropic coordinate model, the vertical component of vorticity may only change through the divergence term in the vorticity equation. The tilting of horizontal vorticity into vertical vorticity resides implicitly in the changing slopes of isentropic surfaces. The solenoidal production term is absent because pressure and density gradients are parallel on isentropic surfaces. The nondimensional primitive equation vorticity theorem in isentropic coordinates reduces to

$$\frac{D\zeta}{Dt} = -d_a(1 + \zeta), \tag{1}$$

where

$$\zeta = \frac{\partial v}{\partial x} - \frac{\partial u}{\partial y}, \tag{2}$$

$$d_a = \frac{\partial u}{\partial x} + \frac{\partial v}{\partial y}, \tag{3}$$

are the vertical component of vorticity and the horizontal divergence respectively,

$$\frac{D}{Dt} = \frac{\partial}{\partial t} + (u_g + u_a)\frac{\partial}{\partial x} + (v_g + v_a)\frac{\partial}{\partial y} \quad (4)$$

in an adiabatic flow, and the subscripts denote geostrophic and ageostrophic quantities. The vorticity theorem (1) states that relative vorticity is changed by the convergence or divergence of absolute vorticity filaments, which are material lines oriented parallel to the vector vorticity (Gill 1982, p. 228).

Quasi-geostrophic and semigeostrophic vorticity theorems represent two different approximations of (1). The quasigeostrophic isentropic vorticity theorem is expressed as

$$\frac{D\zeta_g}{Dt} = -d_a, \quad (5)$$

where

$$\frac{D}{Dt} = \frac{\partial}{\partial t} + u_g\frac{\partial}{\partial x} + v_g\frac{\partial}{\partial y}. \quad (6)$$

Here, the convergence of planetary vorticity filaments changes the geostrophic relative vorticity, because the relative vorticity $\zeta \ll 1$ and the ageostrophic relative vorticity $\zeta_a \ll \zeta_g$ are comparatively small (Pedlosky 1987, p. 90). As a consequence, cyclonic relative vorticity enhancements are weaker, and anticyclonic enhancements are stronger, than they would be if relative vorticity filaments were advected as well. This is one of the major drawbacks of quasigeostrophic theory that has been partially corrected in semigeostrophic theory.

The semigeostrophic analogue of (1) and (5) is derived in terms of the vorticity, divergence, and shearing and stretching deformation theorems presented in I. These are given respectively by

$$\frac{D\zeta_g}{Dt} = -d_a\left(1 + \frac{\zeta_g}{2}\right) + \frac{\tau_g\eta_a - \eta_g\tau_a}{2}, \quad (7)$$

$$0 = -\zeta_a\left(1 + \frac{\zeta_g}{2}\right) + \frac{\tau_g\tau_a + \eta_g\eta_a}{2} + \frac{\gamma_g^2 - \zeta_g^2}{2}, \quad (8)$$

$$\frac{D\eta_g}{Dt} = -\tau_a\left(1 + \frac{\zeta_g}{2}\right) + \frac{\tau_g\zeta_a - \eta_g d_a}{2}, \quad (9)$$

$$\frac{D\tau_g}{Dt} = \eta_a\left(1 + \frac{\zeta_g}{2}\right) - \frac{\tau_g d_a + \eta_g\zeta_a}{2}, \quad (10)$$

where the quantities

$$\eta = \frac{\partial v}{\partial x} + \frac{\partial u}{\partial y}, \quad (11)$$

$$\tau = \frac{\partial u}{\partial x} - \frac{\partial v}{\partial y}, \quad (12)$$

represent the shearing and stretching deformations, and D/Dt is given by (4). These expressions can be manipulated to yield

$$\frac{D\beta_g}{Dt} = -d_a(1 + \beta_g), \quad (13)$$

where

$$\beta_g = \zeta_g - \frac{\gamma_g^2 - \zeta_g^2}{4}. \quad (14)$$

Here, (13) represents the semigeostrophic analogue of a vorticity theorem, and β_g represents the analogue of the geostrophic vorticity. Both geostrophic vorticity ζ_g and total deformation $\gamma_g = \sqrt{\eta_g^2 + \tau_g^2}$ appear in this theorem, which illustrates that these quantities appear to be inseparable in the semigeostrophic system. Blumen (1981) has derived a similar result. Here, β_g is just the geostrophic vorticity, modified by the last term in (14), which is retained in order to preserve the conservation properties of the semigeostrophic equations. Hoskins (1975) and Hoskins and Draghici (1977) have pointed out that this last term is small, consistent with the geostrophic momentum approximation, so that (13) is approximated by

$$\frac{D\zeta_g}{Dt} = -d_a(1 + \zeta_g), \quad (15)$$

in this semigeostrophic model. According to (15), the convergence of planetary *and* geostrophic relative vorticity filaments changes the geostrophic relative vorticity in a semigeostrophic model. The presence of ζ_g on the right hand side of (15) ameliorates the deficiency in the quasi-geostrophic vorticity theorem (5) that was discussed above.

Ageostrophic quantities are *not predicted* in semigeostrophic theory. Rather, they influence the motion through their presence in, for example, the time derivative (4). Changes in the ageostrophic vorticity in (8) arise primarily from the changes in the geostrophic vorticity ζ_g and deformation γ_g that are described by (9), (10), and (15). This dependency may be evaluated by differentiating (8) in time, yielding

$$\frac{D\zeta_a}{Dt} \approx \gamma_g\frac{D\gamma_g}{Dt} - \zeta_g\frac{D\zeta_g}{Dt} + \frac{1}{2}\left[\tau_a\frac{D\tau_g}{Dt} + \eta_a\frac{D\eta_g}{Dt} - \zeta_a\frac{D\zeta_g}{Dt}\right], \quad (16)$$

where all ageostrophic time changes have been neglected on the right hand side, consistent with the geostrophic momentum approximation. Substitution of the leading order expressions

$$\frac{D\zeta_g}{Dt} \approx -d_a, \quad \frac{D\tau_g}{Dt} \approx \eta_a, \quad \frac{D\eta_g}{Dt} \approx -\tau_a, \quad (17)$$

derived from (7)–(10), and use of (15), yields

$$\frac{D\zeta_a}{Dt} \approx \frac{d_a}{2}(\zeta_g + \zeta_a). \tag{18}$$

Convergence ($d_a < 0$) coupled with geostrophic anticyclonic vorticity ($\zeta_g < 0$) will spin up ageostrophic cyclonic vorticity according to (18). This relationship is partially responsible for the isolated regions of cyclonic vorticity appearing in Fig. 9a of I. However, *convergence of ageostrophic cyclonic vorticity filaments actually diminishes ageostrophic cyclonic vorticity* according to (18). As a consequence, the lee cyclogenesis mechanism proposed by McGinley (1982) may be limited in its ability to provide significant vortex spinup in a semigeostrophic model. In particular, the lee-side isolated region of cyclonic vorticity appearing in I can *not* be enhanced by vortex tube stretching. This limitation, among other characteristic features of a semigeostrophic model, is illustrated in the numerical simulation presented below.

3. Model

The vortex tube stretching mechanism discussed above is evaluated with a modified version of the semigeostrophic model used in I. The flow is inviscid, hydrostatic, and adiabatic. The potential vorticity distribution in the present model is *nonuniform*. A disturbance in the geopotential and the potential vorticity is introduced upstream of the mountain. This disturbance is advected toward an isolated mountain $z = h(x, y)$ by the basic state deformation flow. The vertical coordinate z is the pseudoheight

$$z = z_0\left[1 - \left(\frac{p}{p_0}\right)^{R/c_p}\right], \tag{19}$$

introduced by Hoskins and Bretherton (1972), where $z_0 = c_p\theta_0/g \approx 30$ km represents the top of the atmosphere ($p = 0$).

The kinematic boundary conditions

$$w = \mathbf{v}\cdot\nabla h, \quad z = h(x, y), H(x, y) \tag{20}$$

may be satisfied on the lower and upper boundaries in an adiabatic flow by choosing isentropic boundaries, as in I. While this choice excludes the presence of boundary potential temperature anomalies such as surface fronts, the implementation of the boundary conditions in a numerical simulation is considerably simplified. The *rigid* upper boundary profile $H(x, y)$ is chosen to coincide with an upper-level isentropic surface from the steady solution presented in I. The rigid upper boundary will not significantly affect the results of the time-dependent model since the vortex spinup mechanisms discussed above should be greatest in the lower half of the flow. The mountain profile $h(x, y)$ is the same as in I.

The equations governing the flow are the semigeostrophic Boussinesq nondimensional equations, expressed in isentropic coordinates. These are the horizontal momentum equations

$$\frac{Du_g}{Dt} - (v_g + v_a) = -\frac{\partial\Psi}{\partial x}, \tag{21}$$

$$\frac{Dv_g}{Dt} + (u_g + u_a) = -\frac{\partial\Psi}{\partial y}, \tag{22}$$

the hydrostatic equation

$$\frac{\partial\Psi}{\partial\Theta} = \Pi, \tag{23}$$

and the continuity equation

$$\frac{\partial}{\partial t}\left(\frac{\partial z}{\partial\Theta}\right) + \frac{\partial}{\partial x}\left(u\frac{\partial z}{\partial\Theta}\right) + \frac{\partial}{\partial y}\left(v\frac{\partial z}{\partial\Theta}\right) = 0. \tag{24}$$

Geostrophic balance is given by

$$u_g = -\frac{\partial\Psi}{\partial y}, \tag{25}$$

$$v_g = \frac{\partial\Psi}{\partial x}. \tag{26}$$

A Rossby number Ro = 0.3 has been absorbed into the geostrophic streamfunction $\Psi = \phi + \Theta\Pi$, where, Ψ is the Montgomery streamfunction, ϕ is the geopotential, and Θ is the potential temperature. The pseudoheight z, given by (19), is nondimensionalized by the deformation depth D. The Exner function Π, nondimensionalized by gD/Θ_0, is expressed as

$$\Pi = \Upsilon p^{R/c_p}, \tag{27}$$

where $\Upsilon = c_p\Theta_0/gD$, the pressure p is nondimensionalized by the reference pressure p_0, and R is the gas constant for dry air. The relationship between the Exner function and the pseudoheight z is simply

$$\Pi = \Upsilon - z. \tag{28}$$

Here, Υ represents the nondimensional top of the atmosphere in units of z.

The conservation of potential vorticity, derived from (15) and (24), is expressed as

$$\frac{Dq_g}{Dt} = 0, \tag{29}$$

where the semigeostrophic potential vorticity in isentropic coordinates is conveniently represented by (Buzzi et al. 1981)

$$q_g = -\left(1 + \frac{\partial^2\Psi}{\partial x^2} + \frac{\partial^2\Psi}{\partial y^2}\right)\Big/\frac{\partial^2\Psi}{\partial\Theta^2}. \tag{30}$$

Rewriting (30) as

$$\frac{\partial^2\Psi}{\partial x^2}+\frac{\partial^2\Psi}{\partial y^2}+q_g\frac{\partial^2\Psi}{\partial\Theta^2}=-1 \tag{31}$$

yields an equation for the geostrophic streamfunction Ψ (Hoskins et al. 1985). For a given *positive* potential vorticity distribution $q_g(x, y, \Theta, t)$, (31) is a linear elliptic partial differential equation that may be solved for Ψ. A basic state solution, corresponding to a deformation flow and uniform stratification ($\Theta = z$), is provided by

$$\bar{\Psi}=\frac{\alpha}{1+\alpha^2}\left[xy+\frac{\alpha}{2}\left(\frac{3+\alpha^2}{1-\alpha^2}x^2-y^2\right)\right]-\frac{(\Upsilon-\Theta)^2}{2}, \tag{32}$$

so that the perturbation streamfunction Ψ' associated with the mountain circulation and the upper level disturbance is a solution of

$$\frac{\partial^2\Psi'}{\partial x^2}+\frac{\partial^2\Psi'}{\partial y^2}+q_g\frac{\partial^2\Psi'}{\partial\Theta^2}=q_g-\bar{q}_g, \tag{33}$$

where $\bar{q}_g$ is the constant potential vorticity associated with (32).

An ageostrophic streamfunction may also be introduced. Following the derivation of Hoskins and Draghici (1977), the continuity equation (24) may be written as

$$\frac{\partial}{\partial x}\left(u_a\frac{\partial z}{\partial\Theta}\right)+\frac{\partial}{\partial y}\left(v_a\frac{\partial z}{\partial\Theta}\right)+\frac{\partial w^*}{\partial\Theta}=0, \tag{34}$$

where the partial Lagrangian vertical velocity w^* is given by

$$w^*=\frac{\partial z}{\partial t}+u_g\frac{\partial z}{\partial x}+v_g\frac{\partial z}{\partial y}. \tag{35}$$

Differentiation of (21) and (22) with respect to Θ, use of the thermal wind relation

$$\frac{\partial\mathbf{v}_g}{\partial\Theta}=\hat{k}\times\nabla\Pi, \tag{36}$$

and the definitions (27) and (35) yield

$$-\frac{\partial w^*}{\partial x}+\frac{\partial}{\partial\Theta}\left[u_a\left(1+\frac{\partial v_g}{\partial x}\right)+v_a\frac{\partial v_g}{\partial y}\right]=Q_1, \tag{37}$$

$$-\frac{\partial w^*}{\partial y}+\frac{\partial}{\partial\Theta}\left[-u_a\frac{\partial u_g}{\partial x}+v_a\left(1-\frac{\partial u_g}{\partial y}\right)\right]=Q_2. \tag{38}$$

The terms

$$(Q_1, Q_2)=\left(2\frac{\partial\mathbf{v}_g}{\partial x}\cdot\nabla\Pi, 2\frac{\partial\mathbf{v}_g}{\partial y}\cdot\nabla\Pi\right) \tag{39}$$

force the ageostrophic motion, as discussed by Hoskins et al. (1978). Thermal wind balance is upset by these forcing terms through convergence and rotation of thermal gradients by the geostrophic wind $\mathbf{v}_g$. Many authors (e.g., Hoskins 1982) have discussed how this ageostrophic circulation restores thermal wind balance.

The continuity equation (34) is satisfied by introducing the vector streamfunction $\boldsymbol{\psi}=(\psi_1, \psi_2)$, where

$$u_a\frac{\partial z}{\partial\Theta}=\frac{\partial\psi_1}{\partial\Theta}, \tag{40}$$

$$v_a\frac{\partial z}{\partial\Theta}=\frac{\partial\psi_2}{\partial\Theta}, \tag{41}$$

$$\omega^*=-\nabla\cdot\boldsymbol{\psi}, \tag{42}$$

Substituting (40)–(42) into (37) and (38) yields

$$\frac{\partial^2\psi_1}{\partial x^2}+\frac{\partial}{\partial\Theta}\left[\left(1+\frac{\partial v_g}{\partial x}\right)\Big/\frac{\partial z}{\partial\Theta}\right]\frac{\partial\psi_1}{\partial\Theta}+\left[\left(1+\frac{\partial v_g}{\partial x}\right)\Big/\frac{\partial z}{\partial\Theta}\right]\frac{\partial^2\psi_1}{\partial\Theta^2}=Q_1-\frac{\partial}{\partial x}\left[\frac{\partial\psi_2}{\partial y}\right]-\frac{\partial}{\partial\Theta}\left[\frac{\partial\psi_2}{\partial\Theta}\frac{\partial v_g}{\partial y}\Big/\frac{\partial z}{\partial\Theta}\right], \tag{43}$$

$$\frac{\partial^2\psi_2}{\partial y^2}+\frac{\partial}{\partial\Theta}\left[\left(1-\frac{\partial u_g}{\partial y}\right)\Big/\frac{\partial z}{\partial\Theta}\right]\frac{\partial\psi_2}{\partial\Theta}+\left[\left(1-\frac{\partial u_g}{\partial y}\right)\Big/\frac{\partial z}{\partial\Theta}\right]\frac{\partial^2\psi_2}{\partial\Theta^2}=Q_2-\frac{\partial}{\partial y}\left[\frac{\partial\psi_1}{\partial x}\right]+\frac{\partial}{\partial\Theta}\left[\frac{\partial\psi_1}{\partial\Theta}\frac{\partial u_g}{\partial x}\Big/\frac{\partial z}{\partial\Theta}\right], \tag{44}$$

which are analogous to the Sawyer–Elliasen cross-frontal circulation equations (Sawyer 1956; Elliasen 1959). The coefficients of (43) and (44) may be calculated from the geostrophic streamfunction Ψ, and these equations are linear in ψ_1 and ψ_2. They form a coupled set of elliptic partial differential equations when

$$\left(1+\frac{\partial v_g}{\partial x}\right), \left(1-\frac{\partial u_g}{\partial y}\right)>0, \tag{45}$$

which implies inertial stability, and

$$\frac{\partial z}{\partial\Theta}>0, \tag{46}$$

which implies convective stability.

A time-marching scheme is developed from (29), (33), and (43)–(44). With an initial distribution of positive potential vorticity, (33) is solved for the geostrophic streamfunction Ψ' by means of a three-dimensional multigrid method (Adams 1988). The Exner function Π and the geostrophic velocity $\mathbf{v}_g$ may be calculated from (23), (25), and (26). Then, the coefficients of (43) and (44) may be computed, and these

coupled equations may be iteratively solved to obtain the ageostrophic streamfunction ψ, and from (40)–(42), the ageostrophic velocity. Advection of the potential vorticity field may then be carried out according to (29) by means of a semi-Lagrangian advection scheme (Bates and McDonald 1982). This procedure may be repeated indefinitely, and represents a clear and concise example of how potential vorticity dynamics (Hoskins et al. 1985) may be used to investigate the motion in the present problem.

4. Model results

The vortex stretching mechanism discussed by McGinley (1982) and in section 2 may be evaluated with the model described above by advecting a potential vorticity disturbance over an orographic barrier. A two-dimensional disturbance in the geopotential is chosen to approximate a typical upstream potential vorticity distribution observed prior to the initiation of lee cyclogenesis (Bleck and Mattocks 1984). This disturbance is injected into the basic deformation flow, upstream of an isolated mountain, at $t = 0$. The initial disturbance is given by

$$\phi' = A[1 - \tanh(Bx)][1 - \cos(Cz)], \quad (47)$$

where A, B, and C are constants that are chosen such that the disturbance is inertially and convectively stable,

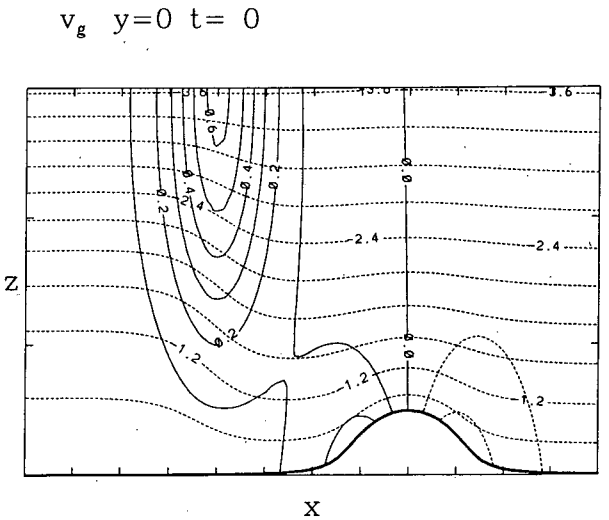

FIG. 1. The initial geostrophic velocity component v_g in the plane $y = 0$. The basic deformation flow has been subtracted out, leaving only the jet (29) and the mountain anticyclone. Positive values (solid contours) indicate flow into the page. The contour value is 0.1, corresponding to a dimensional interval of 3 m s^{-1}. Lightly dashed lines represent isentropes at intervals of 0.3, corresponding to a dimensional interval of approximately 3°K. The heavy contour represents the mountain surface. Tick marks along the x-axis indicate distance in units of mountain half-widths of roughly 333 km. Tick marks along the Θ-axis indicate height z in deformation depths of roughly 3 km.

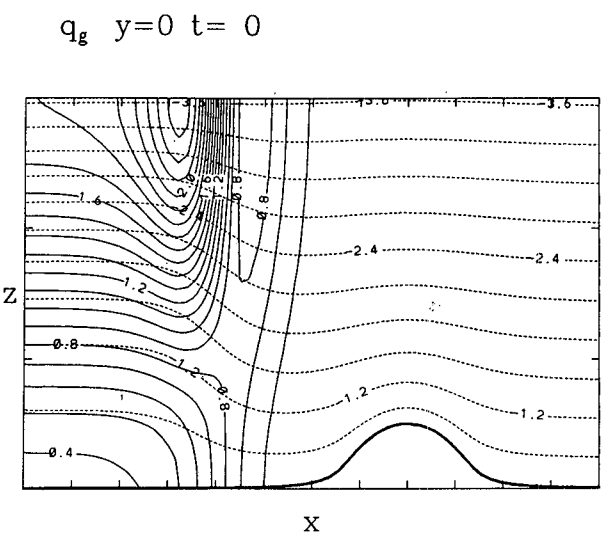

FIG. 2. As in Fig. 1, except for the initial potential vorticity distribution. The contour interval is 0.2, corresponding to a dimensional interval of 2×10^{-7} m^2 s^{-1} K kg^{-1}.

and the potential vorticity is positive. A southerly jet, given by

$$v_g' = \frac{\partial \phi'}{\partial x} = -AB \ \mathrm{sech}^2(Bx)[1 - \cos(Cz)], \quad (48)$$

and a potential temperature distribution characterizing a cold front, given by

$$\theta' = \frac{\partial \phi'}{\partial z} = AC[1 - \tanh(Bx)] \sin(Cz) \quad (49)$$

are associated with the disturbance (47) when $A < 0$.

The initial position of the jet (48) is shown in Fig. 1, and the potential vorticity disturbance, obtained by substituting (47) into (30), is shown in Fig. 2. This potential vorticity distribution corresponds roughly to the leading edge of the quasi-two-dimensional region of high potential vorticity air approaching the Alps prior to the major lee cyclogenesis event of 5 March 1982, (see Bleck and Mattocks 1984, Fig. 2). The initial vertical velocity associated with (47) is shown in Fig. 3. Rising motion ahead of the disturbance and on the windward slope, and sinking motion behind the disturbance and in the lee, are clearly illustrated. This circulation maintains thermal wind balance as the frontal temperature gradient is changed by the basic state deformation through the forcing terms (Q_1, Q_2) defined in (39). A by-product of the isentropic lower boundary condition is a region of diminished static stability behind the disturbance near the ground. This low static stability is a typical feature associated with cold fronts (Keyser 1986). An example, derived from ALPEX data and associated with the lee cyclogenesis event of 4 March 1982, is shown in Fig. 4.

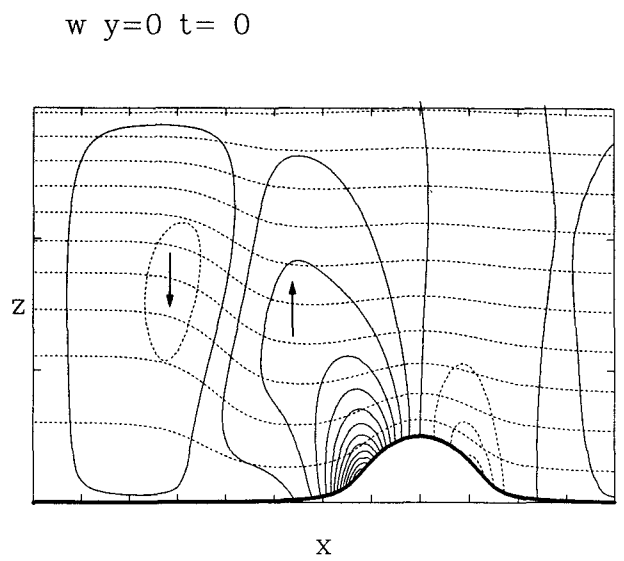

FIG. 3. As in Fig. 1, except for the initial vertical velocity w. Dashed lines indicate downward motion. The contour interval is 0.02, corresponding to a dimensional interval of 0.2 cm s^{-1}.

The initial geostrophic vorticity distribution along the lower boundary, shown in Fig. 5, displays a prominent mountain anticyclone. This feature arises from vortex tube compression associated with flow over the mountain (Smith 1979), and has been discussed in detail by Blumen and Gross (1987b) and in I. Additionally, two isolated lobes of relatively weak cyclonic vorticity are present on the sides of the mountain. These lobes are neglected in the analytical solution provided in I, but they are retained here in order to consistently calculate the vorticity and the solutions to (33), (43), and (44), by means of finite differences. Further, the constant vorticity associated with the basic flow (32), given by $\bar{\zeta}_g/f = 2\alpha^2/(1-\alpha^2) \approx 0.083$, is also included in the distribution shown in Fig. 5. The geostropic vorticity associated with the approaching disturbance is initially zero at the ground.

Vortex spinup is isolated by examining the change in relative vorticity as the disturbance progresses over the isolated mountain. This change is calculated by subtracting the initial vorticity distribution, shown in Fig. 5, from subsequent vorticity fields. The net vor-

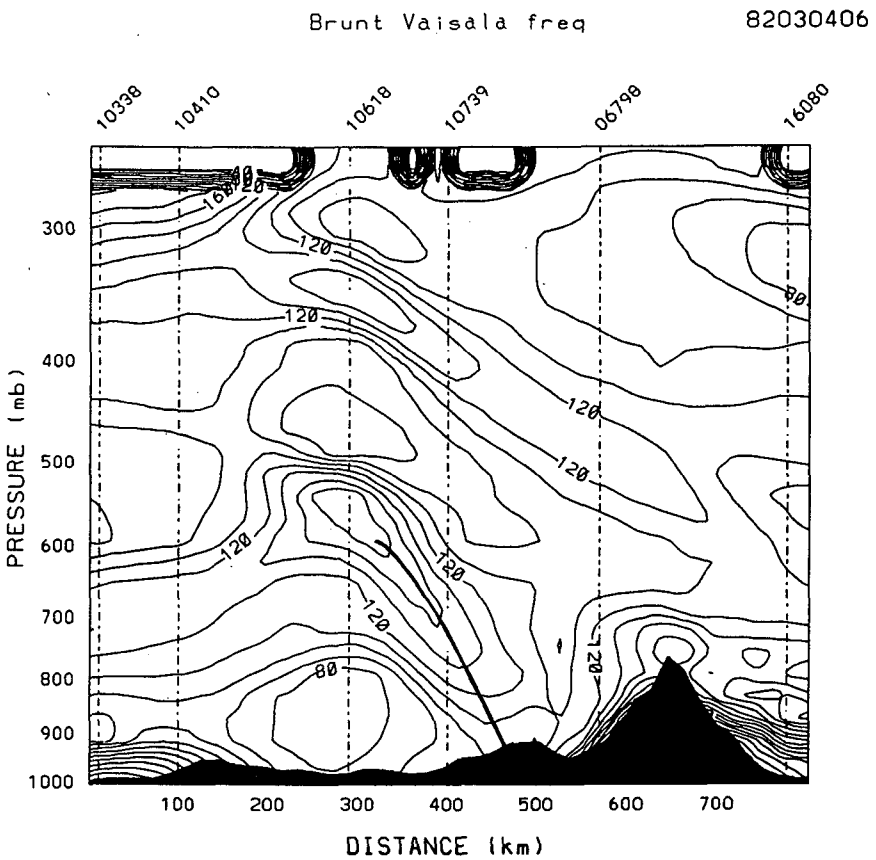

FIG. 4. Analysis of the Brunt–Väisälä frequency associated with a cold front approaching the Alps on 4 March 1982. Units are 10^{-4} s^{-1}. The heavy solid line indicates the position of the front near the surface.

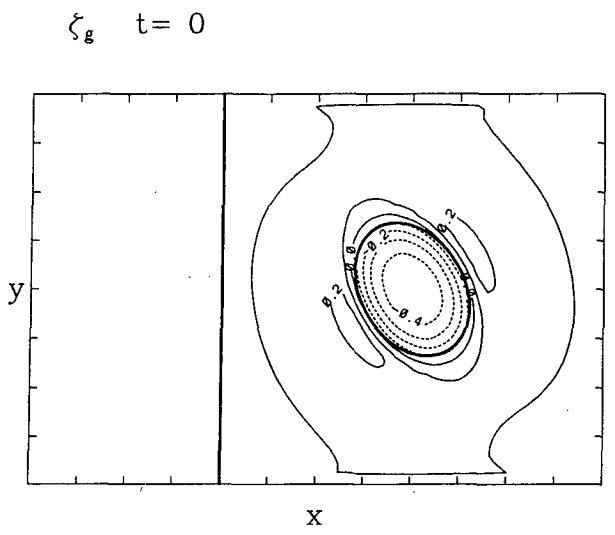

FIG. 5. The initial distribution of the vertical component of geostrophic vorticity along the lower boundary. The contour interval is 0.1, corresponding to 10^{-5} s^{-1}. The heavy ellipse indicates the mountain half-width. The heavy line indicates a potential vorticity contour along the lower boundary, located at the center of the disturbance displayed in Fig. 3. Tick marks along the x- and y-axes indicate distance in units of mountain half-widths of roughly 333 km. The basic state deformation flow is from the west-northwest.

ticity after eighty hours have elapsed is displayed in Fig. 6. There are several features illustrated in Fig. 6 that are associated with vortex spinup as described by (15). A quasi-two-dimensional region of cyclonic vorticity has appeared ahead of the disturbance, and anticyclonic vorticity has appeared behind it. Initially, there is a region of weak convergence ahead of the disturbance and weak divergence behind it. Consequently, cyclonic vorticity is produced ahead of the disturbance and anticyclonic vorticity is produced behind it, according to (15).

Rapid spindown occurs over the mountain as the disturbance progresses over the region of strong divergence shown in Fig. 9 of I. This divergence is associated with vortex-tube compression and the maintenance of the mountain anticyclone in the steady solution. As a consequence, a prominent gap appears in the net cyclonic vorticity distribution ahead of the disturbance. Further, weak cyclonic vorticity appears over the mountain after the passage of the disturbance, indicating a weaker mountain anticyclone than the one displayed in Fig. 5. This diminished anticyclonic vorticity is a direct consequence of the decreased static stability N, and the consequently smaller nondimensional mountain height $\epsilon/D = \epsilon N/fL$, behind the disturbance near the ground, shown in Fig. 1. As the static stability decreases, vortex tube compression over the mountain also decreases, yielding a weaker mountain anticyclone. The ageostrophic mountain circulation also decreases with the static stability, since the stratification acts as a rigid lid (Blumen and Gross 1986). Smaller values of N promote slower ageostrophic motion u_a over the mountain, and by continuity, smaller vertical motions as well.

The disturbance is quickly advected around the northern end of the mountain, while the disturbance is retarded at the southern end of the mountain. This type of advection pattern was also produced by Blumen and Gross (1987b), and results from advection by the mountain anticyclone. Further, the cyclonic vorticity associated with the disturbance appears stronger, with magnitude of about 3×10^{-5} s^{-1}, and more concentrated than the trailing anticyclonic vorticity, at the southern end of the mountain. Anticyclonic vorticity is stronger at the northern end of the mountain. These features are a consequence of the vorticity forcing encountered along parcel trajectories, according to (15). For example, parcels encounter exactly equal and opposite amounts of vorticity forcing as they pass over the mountain in the steady solution presented in I, so that no net vorticity is generated. Here, the circulation associated with the disturbance changes these trajectories so that the net vorticity forcing is nonzero. Parcels passing through the divergence maximum near the northern end of the mountain (see Fig. 9d in I) encounter relatively strong anticyclonic vorticity production. Conversely, parcels passing through the convergence maximum near the southern end of the mountain encounter relatively strong cyclonic vorticity production.

A distinct lee cyclone is markedly absent in Fig. 6. The vertical motion and stretching mechanism in this

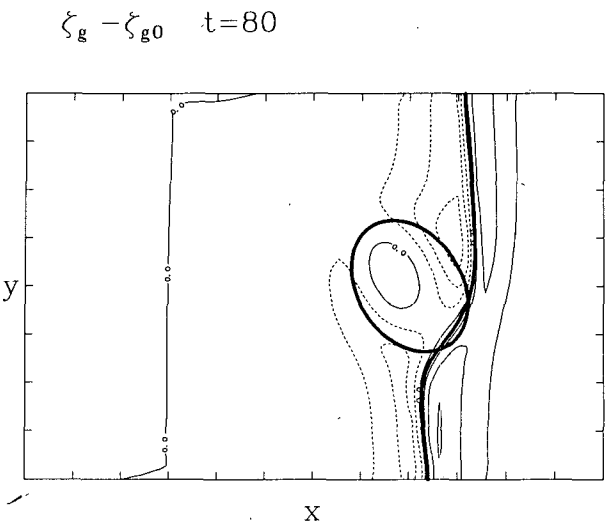

FIG. 6. The net vertical component of geostrophic vorticity along the lower boundary, eighty hours after the initial distribution shown in Fig. 5. The contour interval is 0.1. The heavy ellipse indicates the mountain half-width. The heavy line indicates a potential vorticity contour, initially located at the center of the disturbance.

example are too weak to produce a lee cyclone. As the disturbance passes into the lee, vortex tube stretching, characterized by $\partial w/\partial z$, is clearly present at mid-levels, as shown in Fig. 7, however it is relatively weak. This weak stretching results directly from the passage of the weakly stratified air behind the disturbance into the lee. Weak stratification effectively reduced the nondimensional mountain height $\epsilon/D = \epsilon N/fL$. As a consequence, the mountain anticyclone and the ageostrophic circulation over the mountain are not as strong, as discussed above and by Blumen and Gross (1986). Vortex-tube stretching $\partial w/\partial z$ in the lee at $t = 60$ hours is only about half of that prior to the passage of the disturbance over the mountain. Additionally, the relatively large lee-side ageostrophic vorticity distribution shown in Fig. 9a of I is not effectively stretched in this semigeostrophic model, according to (18). Here, convergence in the lee promotes vortex spindown of the ageostrophic cyclonic vorticity field.

Additional experiments were performed that included elongated ridge profiles with various orientations relative to the flow, and different geopotential disturbances such as a jet streak. In every instance, significant vortex spinup was prevented by the intrusion of weakly stratified air into the lee, as discussed above.

The flow interactions examined here were unable to produce a lee cyclone. It is apparent that the passage of low-level air over the mountain in the experiments discussed above prevents significant vortex spinup by means of vortex tube stretching in a semigeostrophic model. Additionally, this mechanism can not enhance the significant ageostrophic cyclonic vorticity that is initially present in the lee. *In this semigeostrophic isentropic model, vortex-tube stretching alone cannot*

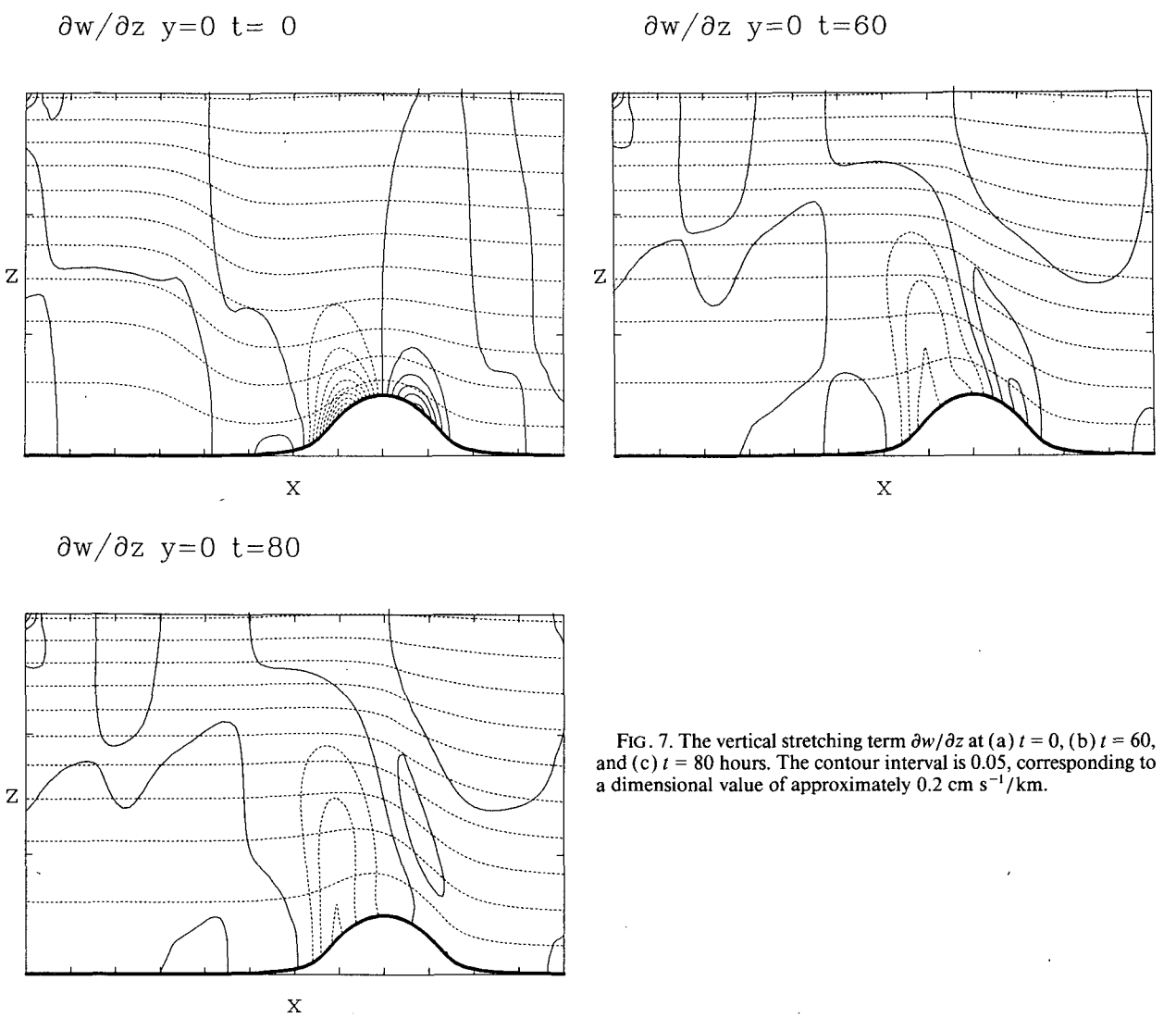

FIG. 7. The vertical stretching term $\partial w/\partial z$ at (a) $t = 0$, (b) $t = 60$, and (c) $t = 80$ hours. The contour interval is 0.05, corresponding to a dimensional value of approximately 0.2 cm s^{-1}/km.

produce a lee cyclone. Further comments are reserved for section 6.

5. Quasi-geostrophic evaluation

A quasi-geostrophic model of flow over the isolated ridge has been examined, for comparative purposes. This model is identical to the semigeostrophic model with the two-dimensional jet (48), except that advection by the ageostrophic velocity has been neglected. The only changes in the governing equations that result from this approximation arise in the Lagrangian time derivative and the diagnostic equations for the ageostrophic velocity (43)–(44). These are given in the quasi-geostrophic model by (6) and

$$\frac{\partial^2\psi_1}{\partial x^2}+\frac{\partial}{\partial\Theta}\left[\left(\frac{\partial z}{\partial\Theta}\right)^{-1}\right]\frac{\partial\psi_1}{\partial\Theta}+\left(\frac{\partial z}{\partial\Theta}\right)^{-1}\frac{\partial^2\psi_1}{\partial\Theta^2}=Q_1-\frac{\partial}{\partial x}\left[\frac{\partial\psi_2}{\partial y}\right] \quad (50)$$

$$\frac{\partial^2\psi_2}{\partial y^2}+\frac{\partial}{\partial\Theta}\left[\left(\frac{\partial z}{\partial\Theta}\right)^{-1}\right]\frac{\partial\psi_2}{\partial\Theta}+\left(\frac{\partial z}{\partial\Theta}\right)^{-1}\frac{\partial^2\psi_2}{\partial\Theta^2}=Q_2-\frac{\partial}{\partial y}\left[\frac{\partial\psi_1}{\partial x}\right]. \quad (51)$$

While the nondimensional mountain height $\epsilon/D = 0.5$ and the Rossby number Ro = 0.3 are too large for a quasi-geostrophic model, these values will be retained in the present analysis for purposes of comparison.

Hoskins has pointed out that a semigeostrophic model simply distorts quasi-geostrophic fields, primarily by concentrating cyclonic vorticity and diluting anticyclonic vorticity. This feature is apparent in a comparison of the quasi-geostrophic net vorticity distribution shown in Fig. 8, and the semigeostrophic distribution shown in Fig. 6. The initial quasi-geostrophic vorticity distribution is identical to the semigeostrophic counterpart because the geostrophic streamfunction equation (31) and the accompanying boundary conditions are the same. However, advection of the potential vorticity distribution, shown in Fig. 2, with only the geostrophic velocity delays the passage of the disturbance over the mountain. In Fig. 8, the disturbance is upstream relative to its position in Fig. 6. The gap in the net vorticity distribution behind the mountain is more noticeable in the quasi-geostrophic model because vortex spin-down over the mountain is stronger in (5) than in (15). Further, the quasi-two-dimensional cyclonic vorticity is slightly weaker and broader, and the anticyclonic vorticity is stronger and more confined, in the quasi-geostrophic solution, as discussed above. The relatively strong quasi-geostrophic cyclonic vorticity near the southern domain boundary is a by-product of a stronger ageostrophic velocity component u_a, derived from the quasi-geostrophic expressions

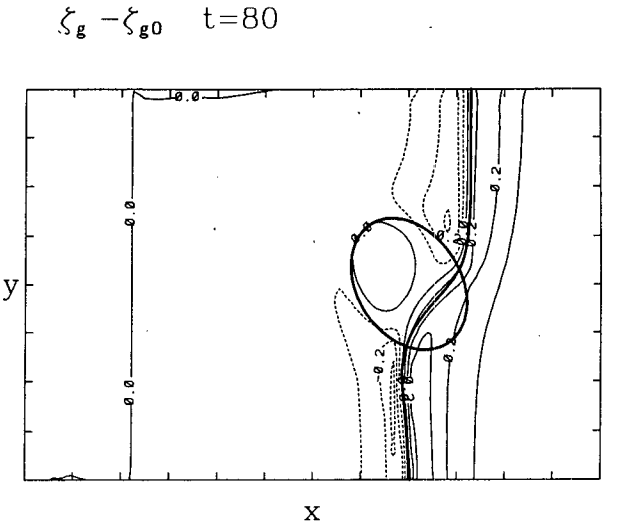

FIG. 8. As in Fig. 6, except for the quasi-geostrophic solution at t = 80 hours.

(50)–(51). According to (22), a stronger disturbance velocity v_g will develop. These features are the only apparent differences between the semigeostrophic and quasi-geostrophic solutions.

Rapid vortex spinup is inhibited in the quasi-geostrophic model by the same mechanism that prevents it in the semigeostrophic model. The introduction of weaker static stability behind the disturbance into the lee reduces the strength of the mountain circulation. Additionally, the quasi-geostrophic vertical velocity and $\partial w/\partial z$ are initially weaker in the lee because the ageostrophic velocity is neglected in the kinematic boundary condition (20). Consequently, the convergence and vortex spinup in the lee are even less in a quasi-geostrophic model than in a semigeostrophic model.

6. Conclusions

Vortex tube stretching has been evaluated as a possible mechanism for lee cyclogenesis. This mechanism was shown to enhance geostrophic cyclonic vorticity and diminish ageostrophic cyclonic vorticity in a semigeostrophic model. These features were illustrated in a numerical simulation in which a potential vorticity disturbance was advected over an isolated mountain and an associated region of ageostrophic cyclonic vorticity. *The stretching mechanism was unable to initiate lee cyclogenesis by the rapid spinup of ambient vorticity in a semigeostrophic model with isentropic boundaries.* Convergence and vortex-tube stretching are clearly present in this semigeostrophic model. However, lee-side convergence of ageostrophic cyclonic vorticity filaments diminishes the ageostrophic cyclonic vorticity, according to the ageostrophic vorticity theorem. Additionally, the intrusion of weakly stratified air over

the mountain and into the lee effectively reduces the nondimensional mountain height ϵ/D and the associated mountain circulation, thereby reducing horizontal convergence associated with the stretching mechanism.

There are three fundamental physical features associated with lee cyclogenesis that are absent in the semigeostrophic model presented here. These are irreversible processes such as friction and diabatic heating, temperature gradients along the lower boundary, and the blocking of air by the mountain. The inviscid and adiabatic assumptions in this presentation exclude certain physical processes that may affect the evolution of the geostrophic vorticity distribution. For example, frictional dissipation of the anticyclonic vorticity acquired by vortex tubes as they ascend the mountain could result in net vortex tube stretching and cyclonic vorticity production as these vortex tubes descend in the lee (Buzzi and Tibaldi 1977). Latent heat release in the updraft ahead of the cold front could enhance the vertical motion and vortex tube stretching as the front interacts with the mountain. Nonconservative effects such as these should be included in more realistic models of lee cyclogenesis.

Boundary temperature gradients in the form of surface fronts could eliminate the region of weakly stratified air behind the disturbance, thereby maintaining the strength of the stretching mechanism if the disturbance propagates over the mountain. These fronts may also interact strongly with the orographic flow field (e.g., Zehnder and Bannon 1988) and may alter the stretching mechanism discussed here by providing significant cyclonic vorticity and an augmented vertical velocity field at lower levels in the flow. Ambient boundary temperature gradients associated with vertical shear in the basic flow could promote the formation of unstable Eady waves. Orographic modification of these waves has been proposed as a possible lee cyclogenesis mechanism (Pierrehumbert 1985; Speranza et al. 1985). However, this mechanism has so far enjoyed only limited success in producing lee cyclones (Egger 1988).

Perhaps a more fundamental modification of the present model would be the introduction of a blocking mechanism that would prevent the weakly stable air from passing over the mountain into the lee. Mesinger and Pierrehumbert (1986) have pointed out that blocking must contribute to any lee cyclogenesis theory, while Pichler and Steinacker (1987) have convincingly demonstrated the importance of blocking in the lee cyclogenesis event of 4–5 March 1982. By preventing the weakly stable air from entering the lee, the stretching mechanism would remain relatively strong, and could initiate lee cyclogenesis. Additionally, upstream blocking may remove the symmetry of flows such as the one considered in I, that exclude any *net* vorticity production as air passes over an obstacle.

Upstream blocking may be introduced by increasing the nondimensional mountain height, representing either an increase in the mountain slope ϵ/L or the characteristic static stability N. The latter effect may be achieved by increasing the ambient static stability, or by replacing the weakly stratified air behind the disturbance with dense, strongly stratified air. However, Pierrehumbert and Wyman (1985) have shown that quasigeostrophic flow is characterized by $\epsilon/D \leqslant 0.1$, while Blumen and Gross (1987b) have shown that semigeostrophic orographic flows are constrained by $\epsilon/D \leqslant 0.5$, the value used in the model presented here. Evidently, nonlinear balanced models such as this one, in which the mountain height is constrained by the geostrophic momentum approximation, cannot properly simulate blocked flow. Indeed, Smith (1989) envisions upstream blocking as the intersection of an isentropic surface with the lower boundary at a stagnation point on the windward slope. However, this configuration is associated with propagating gravity waves, which are absent in balanced models such as the one employed here. Further, it is doubtful that Alpine lee cyclogenesis, characterized by a Rossby number Ro ~ 1, can be properly modeled with either a quasi-geostrophic or semigeostrophic model. A nonlinear primitive equation model that includes realistic boundary profiles and temperature distributions, as well as a blocking mechanism, must be employed (Egger 1988).

Acknowledgments. Financial support for this investigation was provided by the National Science Foundation under NSF Grant ATM 86-17636. The numerical computations were carried out on the Pyramid 90x supermini computer at the University of Colorado Center for Atmospheric Theory and Analysis, and on the Cray X-MP at the National Center for Atmospheric Research, sponsored by the University Corporation for Atmospheric Research. This investigation was part of the author's Ph.D. dissertation, and many thanks are extended to William Blumen, who directed the research and provided pertinent editorial comments for this manuscript. Comments from anonymous reviewers also greatly improved the manuscript. Thanks are also extended to John Adams, at the National Center for Atmospheric Research, for assistance in applying the mutigrid methods employed here, and to Craig Hartsough for Fig. 5.

REFERENCES

Adams, J. C., 1988: MUDPAK: Multigrid software for linear elliptic partial differential equations. [Obtainable from the National Center for Atmospheric Research, Scientific Computing Division, P.O. Box 3000, Boulder, CO 80307.]

Bates, J. R., and A. McDonald, 1982: Multiply-upstream, semi-lagrangian advective schemes: analysis and application to a multilevel primitive equation model. *Mon. Wea. Rev.*, **110**, 1831–1842.

Bleck, R., and C. Mattocks, 1984: A preliminary analysis of the role of potential vorticity in Alpine lee cyclogenesis. *Beitr. Phys. Atmos.*, **57,** 357–368.

Blumen, W., 1981: The geostrophic coordinate transformation. *J. Atmos. Sci.*, **38,** 1100–1105.

——, and B. D. Gross, 1986: Semigeostrophic disturbances in a stratified shear flow over a finite-amplitude ridge. *J. Atmos. Sci.*, **43,** 3077–3088.

——, and ——, 1987a: Advection of a passive scalar over a finite-amplitude ridge in a stratified rotating atmosphere. *J. Atmos. Sci.*, **44,** 1696–1705.

——, and ——, 1987b: Semigeostrophic flow over orography in a stratified rotating atmosphere. Part I: Steady three-dimensional solutions over finite ridges. *J. Atmos. Sci.*, **44,** 3007–3019.

Boyer, D. L., R. Chen and P. A. Davies, 1987: Some laboratory models of flow past the Alpine/Pyrenees mountain complex. *Met. Atmos. Phys.*, **36,** 187–200.

Buzzi, A., and S. Tibaldi, 1977: Inertial and frictional effects on rotating and stratified flow over topography. *Quart. J. Roy. Met. Soc.*, **103,** 135–150.

——, and ——, 1978: Cyclogenesis in the lee of the Alps: a case study. *Quart. J. Roy. Met. Soc.*, **104,** 271–287.

——, A. Trevisan and G. Salustri, 1981: Internal frontogenesis: a two-dimensional model in isentropic, semigeostrophic corrdinates. *Mon. Wea. Rev.*, **109,** 1053–1060.

Chung, Y-S., K. D. Hage and E. R. Reinelt, 1976: On lee cyclogenesis and airflow in the Canadian Rocky Mountains and the East Asian mountains. *Mon. Wea. Rev.*, **104,** 879–891.

Dell'Osso, L., and D. Radinović, 1984: A case study of cyclone development in the lee of the Alps on 18 March 1982. *Beitr. Phys. Atmos.*, **57,** 367–379.

Dutton, J. A., 1986: *The Ceaseless Wind,* Dover Publications, 617 pp.

Egger, J., 1988: Alpine lee cyclogenesis: verification of theories. *J. Atmos. Sci.*, **45,** 2187–2203.

Elliasen, A., 1959: On the formation of fronts in the atmosphere. *The Atmosphere and Sea in Motion.* Rockefeller Institute Press, 277–287.

Gill, A. E., 1982: *Atmosphere-Ocean Dynamics.* Academic Press, 662 pp.

Gross, B. D., and W. Blumen, 1988: Semi-geostrophic flow over orography in a stratified rotating atmosphere. Part II: Some aspects of nonuniform flow over an isolated obstacle. *J. Atmos. Sci.*, **45,** 3003–3015.

Hess, S. L., and H. Wagner, 1948: Atmospheric waves in the northwestern United States. *J. Meteor.*, **5,** 1–19.

Hoskins, B. J., 1975: The geostrophic momentum approximation and the semi-geostrophic equations. *J. Atmos. Sci.*, **32,** 233–242.

——, 1982: The mathematical theory of frontogenesis. *Ann. Rev. Fluid Mech.*, **14,** 131–151.

——, and F. P. Bretherton, 1972: Atmospheric frontogenesis models: mathematical formulation and solution. *J. Atmos. Sci.*, **29,** 11–37.

——, and I. Draghici,. 1977: The forcing of ageostrophic motion according to the semigeostrophic equations and in an isentropic coordinate model. *J. Atmos. Sci.*, **34,** 1859–1867.

——, —— and H. C. Davies, 1978: A new look at the ω-equation. *Quart. J. Roy. Met. Soc.*, **104,** 31–38.

——, M. E. McIntyre and A. W. Robertson, 1985: On the use and significance of isentropic potential vorticity maps. *Quart. J. Roy. Met. Soc.*, **111,** 877–946.

Hu, Q., and E. R. Reiter, 1987: A diagnostic study of explosive cyclogenesis in the lee of the Rocky Mountains. *Met. Atmos. Phys.*, **36,** 161–184.

Huppert, H. E., and K. Bryan, 1967: Topographically generated eddies. *Deep-Sea Res.*, **23,** 655–679.

Keyser, D., 1986: Atmospheric fronts: an observational perspective. *Mesoscale Meteorology and Forecasting,* P. S. Ray, Ed., Amer. Meteor. Soc., 216–258.

McGinley, J., 1982: A diagnosis of Alpine lee cyclogenesis. *Mon. Wea. Rev.*, **110,** 1271–1287.

Malguzzi, P., A. Trevisan and A. Speranza, 1987: Effects of finite height topography on nongeostrophic baroclinic instability: implications to theories of lee cyclogenesis. *J. Atmos. Sci.*, **44,** 1475–1482.

Mattocks, C., and R. Bleck, 1986: Jet streak dynamics and geostrophic adjustment processes during the initial stages of lee cyclogenesis. *Mon. Wea. Rev.*, **114,** 2033–2056.

Mesinger, F., and R. Pierrehumbert, 1986: Alpine lee cyclogenesis: numerical simulation and theory. *Specific Results of the Alpine Experiment,* Vol. I, GARP Pub. Ser. 27, 141–165.

Pedlosky, J., 1987: *Geophysical Fluid Dynamics,* second ed., Springer-Verlag, 710 pp.

Petterssen, S., 1956: *Weather Analysis and Forecasting, Vol. 1,* 2nd ed., McGraw-Hill, 421 pp.

Pichler, H., and R. Steinacker, 1987: On the synoptics and dynamics of orographically induced cyclones in the Mediterranean. *Met. Atmos. Phys.*, **36,** 108–117.

Pierrehumbert, R. T., 1985: A theoretical model of orographically modified cyclogenesis. *J. Atmos. Sci.*, **42,** 1244–1258.

——, and B. Wyman, 1985: Upstream effects of mesoscale mountains. *J. Atmos. Sci.*, **42,** 977–1003.

Radinović, D., 1965: On forecasting in the West Mediterranean and other areas bounded by mountain ranges by baroclinic model. *Arch. Meteorol. Geophys. Bioklim.* **A14,** 279–299.

——, 1986: On the development of orographic cyclones. *Quart. J. Roy. Met. Soc.*, **112,** 927–951.

Reiter, E., 1963: *Jet-Stream Meteorology.* The University of Chicago Press, 515 pp.

Sawyer, J. S., 1956: The vertical circulation at meteorological fronts and its relation to frontogenesis. *Proc. Roy. Soc. London,* **A234,** 346–362.

Smith, R. B., 1979: The influence of mountains on the atmosphere. *Advances in Geophysics,* Vol. 21, Academic Press, 87–230.

——, 1984: A theory of lee cyclogenesis. *J. Atmos. Sci.*, **41,** 1159–1168.

——, 1989: Mountain-induced stagnation points in hydrostatic flow. *Tellus,* **41A,** 270–274.

Speranza, A., A. Buzzi, A. Trevisan and P. Malguzzi, 1985: A theory of deep cyclogenesis in the lee of the Alps: modifications of baroclinic instability by localized topography. Part I. *J. Atmos. Sci.*, **42,** 1521–1535.

Sutcliffe, R. C., 1947: A contribution to the problem of development. *Quart. J. Roy. Met. Soc.*, **73,** 370–383.

Zehnder, J. A., and P. R. Bannon, 1988: Frontogenesis over a mountain ridge. *J. Atmos. Sci.*, **45,** 628–644.